ELSEVIER

Thermochimica Acta 343 (2000) 145–150

thermochimica acta

www.elsevier.com/locate/tca

Solid–solid interactions between ZnO and Fe_2O_3 as influenced by Al_2O_3-doping

Hala G. El-Shobaky

Chemistry Department, Faculty of Science, Cairo University, Cairo, Egypt

Received 28 June 1999; accepted 24 September 1999

Abstract

The solid–solid interactions between pure and alumina-doped zinc and ferric oxides have been investigated by using XRD technique. The investigated solids were calcined at 600–900°C. The amounts of alumina were 3, 6 and 9 mol%.

The results obtained showed that Fe_2O_3 interacted readily with ZnO at temperatures starting from 700°C producing zinc ferrite. The degree of reaction propagation increased with temperature. The completion of this reaction required a prolonged heating at temperatures >900°C. Al_2O_3-doping promoted the ferrite formation to an extent proportional to its amount added. Furthermore, the doping process resulted in the formation of $ZnFe_2O_4$ at 600°C. The stimulation effect of Al_2O_3 was evidenced by following up the change of peak heights of certain diffraction lines characteristic for $ZnFe_2O_4$, α-Fe_2O_3 and ZnO phases located at "*d*" spacings of 2.54, 2.69 and 2.47 Å, respectively. The activation energies ΔE of the ferrite formation for pure and variously doped mixed oxide solids were computed. The ΔE values were 73.5, 66.8, 57.3 and 68.8 kJ mol^{-1} for pure mixed oxide solid samples and those doped with 3, 6 and 9 mol% Al_2O_3, respectively. The mechanism of Al_2O_3 doping is discussed.

Keywords: Doping; $ZnFe_2O_4$; Mobility; XRD; Solid–solid interactions

1. Introduction

Most of divalent metal oxides (MO) interact with Fe_2O_3 yielding the corresponding ferrite with the formula MFe_2O_4 [1]. These ferrites are classified according to their structure and properties, into two categories: (1) ferrites possessing cubic spinel structure e.g. Mg, Co, Ni, Cu and Zn and (2) ferrites with other different structures e.g. the ferrites of the alkaline earth elements [2–4]. The spinel-type ferrites are commonly utilized in fine electronic devices owing to their remarkable magnetic and semiconducting properties [1,5–10]. The solid–solid interactions between MO and Fe_2O_3 may be influenced by the prehistory of the parent solids, their ratio and also by the addition of small amounts of certain foreign oxides [11–15].

In zinc ferrite formation [16–20], the reactions of ferric oxide sharply decreases if the temperature of its preparation exceeds 675°C because of its sintering. The mechanism of solid–solid interactions between ZnO and Fe_2O_3 is reported to be diffusion of Fe_2O_3 and ZnO into the initially formed ferrite layer [17–19].

Ferrite formation is highly influenced by doping with foreign cation. Li_2O-doping promotes the formation of nickel ferrite [11], zinc ferrite [14] and cobalt ferrite [15]. The promotion effect of lithium

PII: S0040-6031(99)00356-1

was attributed to an effective increase in the mobility of diffusion of reacting cations.

The Al_2O_3-doping (2.5–10 mol%) of NiO enhances the solid–solid interactions between NiO and α-Fe_2O_3 to produce $NiFe_2O_4$ [12] at temperatures starting from 800°C to an extent proportional to the amount of alumina added. This stimulation effect of $NiFe_2O_4$ formation was attributed to an increase in the mobility of the reacting cations Ni^{2+} and Fe^{3+}, due to creation of cationic vacancies in the doped NiO and Fe_2O_3 solids.

The present work reports the results of a study on the effects of the addition of small amounts of Al_2O_3 on zinc ferrite formation at different temperatures using XRD technique.

2. Experimental

2.1. Materials

Hydrated ferric oxide $Fe_2O_3{\cdot}1.5H_2O$ was precipitated from ferric sulphate (BDH) solution using a dilute NH_4OH solution (0.2 N) at 70°C and pH = 8 as reported by El-Shobaky et al. [13]. The gel obtained was washed with bidistilled water until free from the ammonium and sulphate ions, then dried at 100°C to constant weight.

Equimolar proportions of $Zn(NO_3)_2{\cdot}3H_2O$ and hydrated ferric oxide were mixed, homogenized and subjected to thermal treatment in air at 600–900°C for 6 h. Three doped mixed solid samples were prepared by treating known amounts of zinc nitrate and ferric oxide with calculated amounts of aluminum nitrate dissolved in the least amount of distilled water, dried at 100°C, then calcined at 600–900°C for 6 h. The amounts of aluminum, expressed as Al_2O_3 were 3, 6 and 9 mol%. All the employed chemicals were of analytical grade and supplied by Prolabo.

2.2. Technique

X-ray investigation of pure and doped mixed solids precalcined at 600°C, 700°C, 800°C and 900°C were carried out using a Philips diffractometer (type PW 1390). The patterns were recorded with iron-filtered cobalt radiation ($\lambda = 1.7889$ Å) at 30 kV and 10 mA with a scanning speed of 2° in 2θ min^{-1}.

3. Results and discussion

X-ray diffractograms of pure and doped mixed oxide solids precalcined at various temperatures (600–900°C) were determined. Fig. 1 represents the diffractograms of pure and doped mixed oxide solids calcined at 600°C. Fig. 1 showed that the X-ray patterns of the pure mixed solids consisted entirely of α-Fe_2O_3 and ZnO (hexagonal) with high degree of crystallinity. This indicates the absence of any appreciable solid–solid interaction between α-Fe_2O_3 and

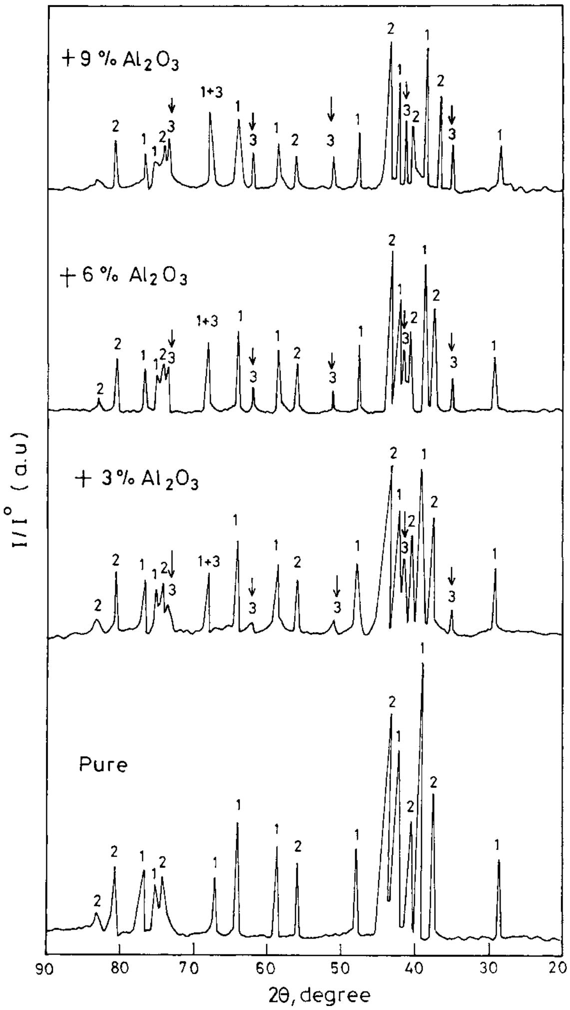

Fig. 1. XRD patterns of pure and doped mixed oxide solids precalcined at 600°C; lines 1 refer to α-Fe_2O_3, lines 2 to ZnO and lines 3 to $ZnFe_2O_4$.

ZnO at 600°C. It can also be observed from Fig. 1 that doping of the investigated mixed oxide solids with 3–9 mol% Al_2O_3 led to the appearance of $ZnFe_2O_4$ phase besides the free oxides. The intensity of diffraction lines of $ZnFe_2O_4$ phase increased as a function of the amount of Al_2O_3 (3–9 mol%). The peak height of the main diffraction line ($d = 2.54$ Å) of zinc ferrite formed at 600°C were 4.5, 8.5 and 9.5 (a.u.) for the mixed oxide solids doped with 3, 6 and 9 mol% Al_2O_3, respectively. i.e., Al_2O_3-doping enhances the solid–solid interaction between α-Fe_2O_3 and ZnO to produce $ZnFe_2O_4$ at 600°C and the degree of enhancement increased as a function of dopant concentration.

The diffractograms of pure and doped mixed oxide solids calcined at 700°C, 800°C (not given here) and 900°C (Fig. 2) consisted of the characteristics diffraction lines of $ZnFe_2O_4$, α-Fe_2O_3 and ZnO phases. Inspection of these diffractograms showed that the relative intensity of the diffraction lines of ferrite phase increased by increasing both calcination temperature and the amount of dopant added. This increase was accompanied by subsequent decrease in the intensity of diffraction lines of α-Fe_2O_3 and ZnO phases. Zinc ferrite is normally produced by interaction between ferric and zinc oxides. The completion of this reaction might require heat treatment of the mixed oxides at elevated temperature [14].

The peak heights of diffraction lines corresponding to $ZnFe_2O_4$, α-Fe_2O_3 and ZnO phases were determined for the various investigated solids preheated at 600–900°C. The results obtained are given in Table 1. It is seen from Table 1 that the peak height of the diffraction lines relative to $ZnFe_2O_4$ phase increased as a function of the calcination temperature and the amount of dopant present with subsequent decrease in the intensity of diffraction lines characteristic to the free oxides. It can be concluded from these results that both temperature and the dopant added stimulated the ferrite formation. The stimulation effect of $ZnFe_2O_4$ formation by doping with Al_2O_3 reached to a maximum limit at 6 mol% Al_2O_3.

The activation energy of formation of $ZnFe_2O_4$ phase (ΔE) at temperatures between 700–900°C for pure and at 600–900°C for doped mixed oxide solids were computed adopting the method suggested by El-Shobaky et al. [11]. The results obtained are given in Table 2. The activation energy of zinc ferrite formation were computed by assuming that the height of the characteristic diffraction lines as a measure of the amount of $ZnFe_2O_4$ present in a given solid sample at a definite temperature (T). This assumption was based on the fact that the diffraction peaks of $ZnFe_2O_4$ phase were sharp for the different solids calcined at 600–900°C and the rise in temperature increased only the relative intensity of these peaks. By plotting the peak height of these lines versus $1/T$, a straight line is obtained, whose slope determines the ΔE value by direct application of the Arrhenius equation. The plots obtained are given in Fig. 3 for two diffraction lines at "d" spacings of 2.54 and 2.96 Å for pure and doped

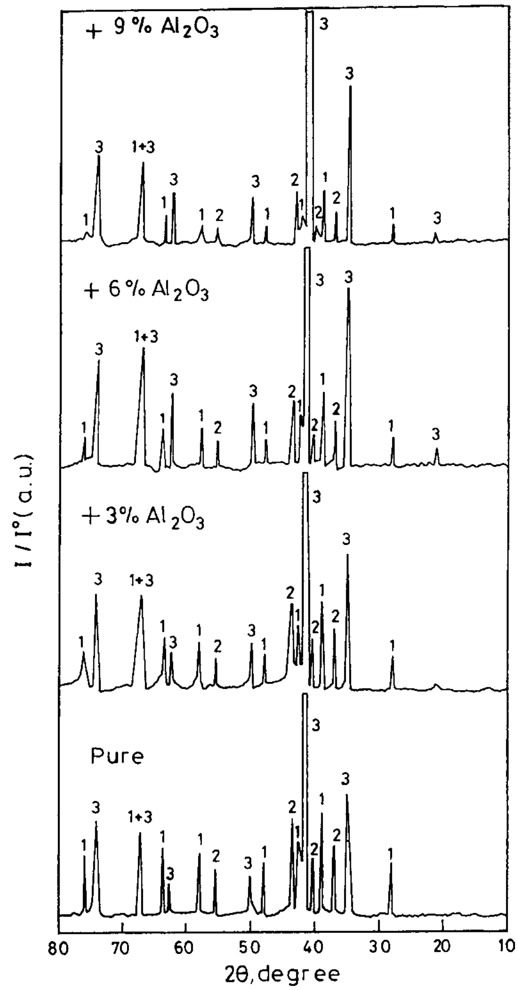

Fig. 2. XRD patterns of pure and doped mixed solids precalcined at 900°C; lines 1 refer to α-Fe_2O_3, lines 2 to ZnO and lines 3 to $ZnFe_2O_4$.

Table 1
The effect of calcination temperature and doping on the height of some characteristic diffraction lines of $ZnFe_2O_4$, α-Fe_2O_3 and ZnO phases

Solid	Calcination temperature (°C)	Height of some diffraction lines (arbitrary units)		
		α-Fe_2O_3 (2.69 Å)	ZnO (2.47 Å)	$ZnFe_2O_4$ (2.54 Å)
Fe_2O_3:ZnO	600	223	184	–
+3% Al_2O_3		136	138	4.5
+6% Al_2O_3		118	122	8.5
+9% Al_2O_3		108	103	9.5
Fe_2O_3:ZnO	700	150	142	9.3
+3% Al_2O_3		127	132	11.5
+6% Al_2O_3		95	105	16.6
+9% Al_2O_3		68	87	11.5
Fe_2O_3:ZnO	800	145	136	19.2
+3% Al_2O_3		102	128	25.2
+6% Al_2O_3		84	91	33.8
+9% Al_2O_3		62	84	20
Fe_2O_3:ZnO	900	107	94	43
+3% Al_2O_3		91	80	52
+6% Al_2O_3		70	60	56
+9% Al_2O_3		58	45	40

mixed oxide solids. The computed ΔE values obtained from the two diffraction lines are close to each other as shown in Table 2. This indicates that alumina-doping enhances the ferrite formation via facilitating diffusion of various reacting species through each other. The maximum decrease in the activation energy of diffusion was found by doping the investigated system with 6 mol% Al_2O_3.

The role of Al_2O_3 in decreasing the activation energy of zinc ferrite formation and consequently enhancing the solid–solid interaction between α-Fe_2O_3 and ZnO may be attributed to the action of Al_2O_3 in increasing the mobility of the reacting cations Fe^{3+} and Zn^{2+}. The induced increase in the mobility due to doping can be explained by discussing the mechanism of dissolution of Al^{3+} ions in α-Fe_2O_3 and ZnO lattices via substitution of some of host Fe^{3+} and Zn^{2+} ions. The substitution process can be simplified by the use of Kröger's notations [21] in the

Table 2
Activation energy of zinc ferrite formation computed from two diffraction lines relative to zinc ferrite

Solid	Activation energy (kJ mol^{-1}) at	
	2.54 Å	2.96 Å
Fe_2O_3:ZnO	73.5	70.6
+3% Al_2O_3	66.8	63.5
+6% Al_2O_3	57.3	57.1
+9% Al_2O_3	68.8	64.1

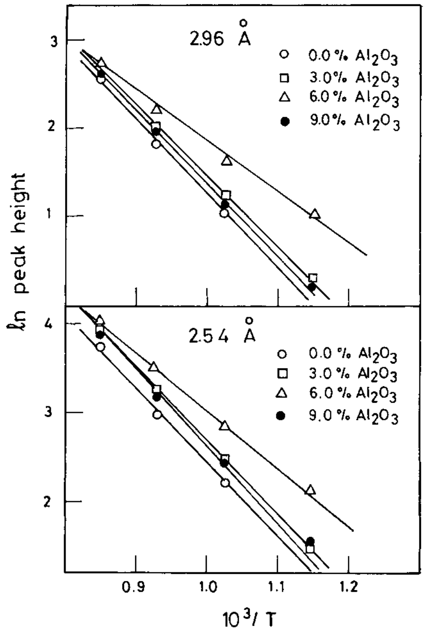

Fig. 3. Variation of ln peak height of different lines of $ZnFe_2O_4$ (2.54 and 2.96 Å) as a function of calcination temperature for pure and Al-doped mixed solids.

following manner:

$$Al_2O_3 \rightarrow 2Al(Fe^{3+}) + C.V. \qquad (1)$$

$$Al_2O_3 \rightarrow 2Al(Zn^{2+}) + 2Zn^{+} \qquad (2)$$

where $Al(Fe^{3+})$ and $Al(Zn^{2+})$ are the trivalent aluminum ions located in the positions of the host cations Fe^{3+} and Zn^{2+} of α-Fe_2O_3 and ZnO lattices, C.V. is cationic vacancy and Zn^{+} is a created monovalent zinc ions located in interstitial position of zinc oxide lattice. The created cationic vacancies might increase the mobility of the reacting Fe^{3+} cations (Eq. (1)). So, Al_2O_3-doping of the investigated mixed oxides led to an increase in the peak height of the different lines of $ZnFe_2O_4$ phase with subsequent decrease in the peak height of the lines of unreacted α-Fe_2O_3 and ZnO phases (c.f. Table 1). The dissolution of Al^{3+} in the α-Fe_2O_3 lattice via substitution mechanism given by Eq. (1) does not affect the concentration of the trivalent Fe^{3+} cations. The dissolution process might only be accompanied by an increase in the mobility of Fe^{3+} ions via creation of cationic vacancies. The role of Al_2O_3 in increasing the mobility of Fe^{3+} ions was previously discussed by El-Shobaky et al. [12] in the case of $NiFe_2O_4$ formation as affected by Al_2O_3-doping, where Al^{3+} ions dissolved in both Fe_2O_3 and NiO lattices via substitution mechanism. However, the degree of enhancement of $NiFe_2O_4$ by action of Al^{3+} ions was much greater than in the present case due to creation of cationic vacancies in both Fe_2O_3 and NiO lattices.

The dissolution of Al_2O_3 in ZnO lattice according to the mechanism given by Eq. (2) led to conversion of some of host Zn^{2+} ions into Zn^{+} (Eq. (2)) decreasing thus the concentration of Zn^{2+} species involved in zinc ferrite formation. The effect of Li_2O-doping in enhancing the solid–solid interaction between ZnO and Fe_2O_3 yielding $ZnFe_2O_4$ should be more pronounced as compared to that manifested by Al_2O_3-doping [14]. As dissolution of Li^{+} ions in ZnO lattice effected transformation of Zn^{+} ions (present in non-stoichiometric oxide calcined at $\geq$500°C) into Zn^{2+} ions. This speculation has been verified experimentally by comparing the published results on Li_2O-doping in $ZnFe_2O_4$ formation [14] to those given in the present work.

The creation of cationic vacancies due to Al_2O_3-doping of α-Fe_2O_3 might be expected to be accompanied by an enhancement of the ferrite formation. However, the conversion of some of Zn^{2+} into Zn^{+} taking place as a result of Al_2O_3-doping of ZnO might oppose slightly the ferrite formation. This speculation comes from the possible induced decrease in the concentration of zinc species involved in $ZnFe_2O_4$ formation. In other words, the dissolution of dopant ions in α-Fe_2O_3 and ZnO lattices according to Eqs. (1) and (2) exerted two opposite effects towards the ferrite formation.

The observed decrease in the activation energy of formation due to Al_2O_3-doping with 3 and 6 mol% (73.5 and 57.3 kJ mol^{-1}) might suggest the domination of the increase in the mobility of trivalent iron cations or dissolution of extremely small amounts of Al^{3+} ions in ZnO lattice treated with 3 and 6 mol% Al_2O_3. The observed increase in ΔE value from 57.3 to 68.8 kJ mol^{-1} by increasing the amount of dopant from 6 to 9 mol% Al_2O_3 could be attributed to dissolution of a significant amount of Al_2O_3 into ZnO lattice according to the mechanism represented by Eq. (2).

4. Conclusions

The main conclusions that can be derived from the obtained results are:

1. Solid–solid interaction between α-Fe_2O_3 and ZnO occurred at temperatures starting from 700°C to produce crystalline $ZnFe_2O_4$ phase. The extent of reaction increased by the calcination temperature in the range 700–900°C. The reaction did not go to completion at 900°C.
2. Alumina-doping promoted the zinc ferrite formation at temperatures starting form 600°C to an extent proportional to its amount present.
3. Raising the calcination temperature from 700°C to 900°C led to an increase in the promotion effect of Al_2O_3-doping which attained its maximum limit at 6 mol%.
4. The activation energy of formation of $ZnFe_2O_4$ for pure and Al_2O_3-doped solids were 73.5, 66.8, 57.3 and 68.8 kJ mol^{-1} for pure mixed oxide solids and those doped with 3, 6 and 9 mol% Al_2O_3, respectively. The promotion effect of $ZnFe_2O_4$ formation due to doping with 3 and 6 mol% Al_2O_3

was attributed, mainly, to dissolution of Al_2O_3 in α-Fe_2O_3 with subsequent creation of cationic vacancies. The increase in the activation energy from 57.3 to 68.8 kJ mol^{-1} by increasing the amount of dopant from 6 to 9 mol% Al_2O_3 might reflect the dissolution of Al_2O_3 added in ZnO lattice leading to conversion of Zn^{2+} to Zn^{+} ions.

References

[1] P. Pascal, Nouveau Traité de Chimie Minérale, Tome II, Masson, Paris, 1966, p. 702.

[2] V.V. Valkov, A. Deneva, D. Stavrakeva, Proc. Seventh Int. Congr. Chem. Cem., Paris, France, vol. 3, 1980, V/98–V/101.

[3] L.M. Letyuk, M.N. Shipko, V.S. Tikhonov, M.V. Dimetriev, Izv. Akad. Nauk SSSR, Neorg. Mater. 18(10) (1980) 340.

[4] K. Tae Ok, K.E. Dong, Yo-op Hoe Chi (Korea) 20(4) (1983) 340.

[5] M.W. Shafer, J. Appl. Phys. 33 (1962) 1210.

[6] N. Yoji, M. Kimio, Patent, Japan, Kokai, Tokkyo Koho, 79, 159 696 (C1-H01F1/34), 17 December 1979, Appl., 78/68 682.

[7] V.V. Pan'Kov, L.A. Bashkiro, Yu.G. Saksonov, Izv. Akad. Nauk SSSR, Neorg. Mater. 15(5) (1978) 922.

[8] T. Mitev, T. Dimova, G. Khristova, Bulg. Sklar Keram. 32(8) (1982) 207.

[9] M. Crisan, D. Crisan, Mater. Sci. Monogr. (Ceram-Powders) 16 (1983) 429.

[10] Fuji Electrochem., Patent, Japan, Kokai, Tokkyo Koho, 59 213 627 (84 213 627) Cl. Clog 53/00, 3 December 1984, Appl. 83/87 046, 8 May 1983.

[11] A.A. Ibrahim, G.A. El-Shobaky, Thermochim. Acta 132 (1988) 117.

[12] G.A. El-Shobaky, A.A. Ibrahim, Bull. Soc. Chem. (France) 1 (1989) 34.

[13] G.A. El-Shobaky, G.A. Fagal, A. Abd.El-Aal, A.M. Ghozza, Thermochim. Acta 256 (1995) 429.

[14] G.A. El-Shobaky, F.H.A. Abdalla, A.A. Fouad Zikry, Thermochim. Acta 289 (1996) 81.

[15] G.A. El-Shobaky, F.H.A. Abdalla, A.M. Ghozza, Thermochim. Acta 292 (1997) 123.

[16] D.W. Hopkins, J. Electrochem. Soc. 96 (1949) 195.

[17] G.A. Kolta, S.Z. El-Tawil, A.A. Ibrahim, N.S. Felix, Thermochim. Acta 36 (1980) 359.

[18] A. Feltz, A. Martin, Mater. Sci. Monogr. (React. Solids) 28A (1985) 137.

[19] F.J.C. Toolenaar, J. Mater. Sci. 24 (1989) 1089.

[20] R. Furichi, K. Tami, K. Kamada, T. Ishci, React. Solids 1 (1986) 309.

[21] F.A. Kröger, Chemistry of Imperfect Crystals, North-Holland, Amsterdam, 1964.